07 - 10 September 2009

PROCEEDINGS

54. IWK

Internationales Wissenschaftliches Kolloquium
International Scientific Colloquium

Information Technology and Electrical Engineering - Devices and Systems, Materials and Technologies for the Future

Faculty of Electrical Engineering and Information Technology

Startseite / Index:
http://www.db-thueringen.de/servlets/DocumentServlet?id=14089

TECHNISCHE UNIVERSITÄT
ILMENAU

Impressum

Herausgeber: Der Rektor der Technischen Universität Ilmenau
Univ.-Prof. Dr. rer. nat. habil. Dr. h. c. Prof. h. c.
Peter Scharff

Redaktion: Referat Marketing
Andrea Schneider

Fakultät für Elektrotechnik und Informationstechnik
Univ.-Prof. Dr.-Ing. Frank Berger

Redaktionsschluss: 17. August 2009

Technische Realisierung (USB-Flash-Ausgabe):
Institut für Medientechnik an der TU Ilmenau
Dipl.-Ing. Christian Weigel
Dipl.-Ing. Helge Drumm

Technische Realisierung (Online-Ausgabe):
Universitätsbibliothek Ilmenau
ilmedia
Postfach 10 05 65
98684 Ilmenau

Verlag:
Verlag ISLE, Betriebsstätte des ISLE e.V.
Werner-von-Siemens-Str. 16
98693 Ilmenau

ISBN (USB-Flash-Ausgabe): 978-3-938843-45-1
ISBN (Druckausgabe der Kurzfassungen): 978-3-938843-44-4

Startseite / Index:
http://www.db-thueringen.de/servlets/DocumentServlet?id=14089

APPLICATION OF ULTRA WIDEBAND RADAR SENSORS FOR NON-DESTRUCTIVE TESTING OF PIPE SYSTEMS AND SALT MINE TUNNELS

F. Bonitz[1], R. Herrmann[1], M.Eidner[2], J. Sachs[1], H.Solas[3]

[1] Ilmenau University of Technology, P.O. Box 100 565, 98684 Ilmenau; [2]Bo-Ra-tec GmbH, Hegelstraße 5, 99423 Weimar; [3]Forschungsinstitut für Tief- und Rohrleitungsbau Weimar e.V., Georg-Haar-Straße 5, 99427 Weimar

ABSTRACT

In this paper we present two non-destructive testing applications of ultra wideband sensors for examination of salt mine tunnels and the inspection of the bedding zone of sewer pipes. The goal is to gain knowledge about the surface near areas and detect inhomogeneities like disaggregation or perturbations. This knowledge allows drawing conclusions for security and quality assessment purposes.
The systems presented here are both based on a 4 GHz bandwidth ultra-wideband radar concept which has been extended according to the application.

Index Terms **-** ultra wideband, radar, sensor, inspection, non-destructive testing, pipe, crack detection, salt mine, quality assurance, m-sequence

1. INTRODUCTION

Ultra wideband sensors can be deployed in many different applications – such as non-destructive testing in civil engineering (NDTCE). This paper presents two different UWB systems for the inspection and quality assessment of salt mine tunnels [1],[5] and sewer pipe systems [2],[3]. In both applications, a cylindrically shaped volume around the pipe or tunnel is the area of particular interest. For example, after laying of sewer pipes a main interest is to get information about the homogeneity of the bedding zone, a zone about 30 cm around the pipe. In salt mines the salt rock surrounding tunnels is known to disaggregate over the years of usage and defects appear roughly up to 1 m inside the rock. These distortions of a normally homogeneous medium are usually very small in size. UWB systems can generally benefit from their high range resolution in such cases. However, other system aspects such as stability/repeatability become more important as target size decreases.

2. UWB SYSTEMS FOR NDTCE

In this paper we consider two different systems both based on the M-sequence approach introduced in [4]. The basic components of an M-sequence system and its assembly are shown in Figure 1. It consists of high frequency circuits integrated in a SiGe:C semiconductor process. Main parts are the M-sequence generator (example depicted in Figure 2) providing the radar stimulus, wideband track & hold circuits for the receivers, a clock divider for synchronisation and a system clock generator. A microcontroller system is used for data capturing and pre-processing. Data is transferred to a PC by a TCP/IP connection. In the presented applications, a 9th order M-sequence is used as stimulus. This results in a period length of 511 master clock cycles. With a typical master clock rate of 9 GHz maximum round trip time of one A-scan is about 56 ns translating into an ambiguity range of about 8.5 m in air. In the next sub-sections, components and mode of operation of the two modified systems are described.

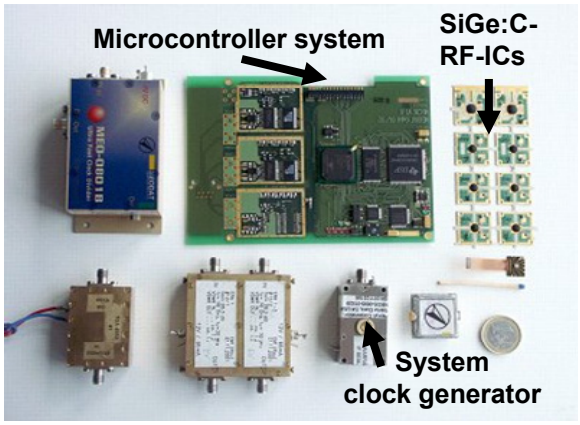

Figure 1: basic components of an M-sequence system

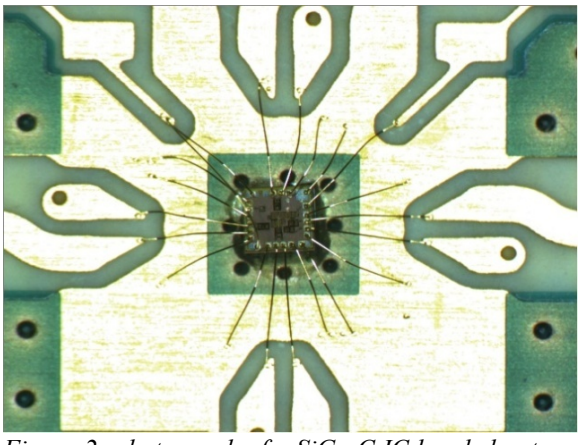

Figure 2: photograph of a SiGe:C IC bonded onto an RF-PCB

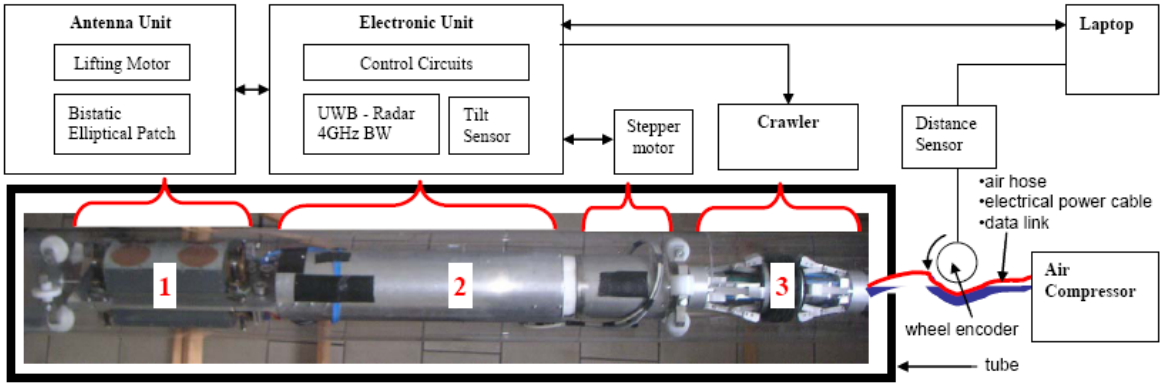

Figure 3: block diagram of the tube crawler prototype. Consisting of these main units: 1-antenna unit, 2-electronic unit, 3-crawler (drive assembly)

2.1. The Tube-Crawler System

The prototype is optimised for usage in sewer pipe systems with a diameter of 200 mm. A block diagram of the whole system is depicted in Figure 3. Basis parts of the system are the antenna unit (1), electronic unit (2) and the drive assembly (3). A short description follows, but for a more detailed review, the reader may refer to [2] and [3].

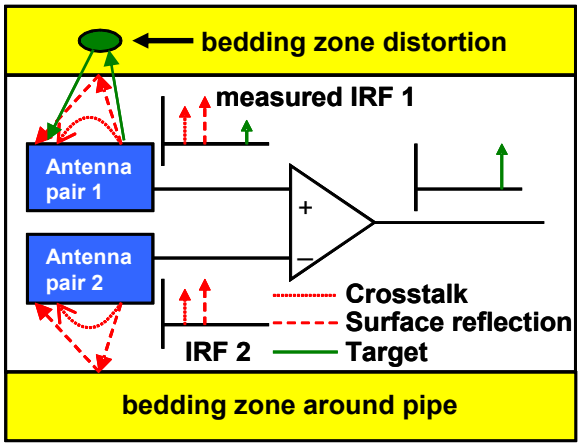

Figure 4: measurement modes of the antenna unit; normal bistatic mode: only antenna pair 1 is used, bistatic differential mode: both pairs are used

2.1.1. Antenna Unit

This part consists of two identical elliptical patch antenna pairs which can be operated in a basic bistatic setup and a differential bistatic mode. The latter principle uses both identical pairs and the idea behind this is shown in Figure 4. The crosstalk of the antennas in each pair and surface reflections from both sides of the tube are very similar and erase each other when taking the difference. In the case of homogenous bedding, antenna pair 1 and antenna pair 2 receive the very same responses and at the output of the differential amplifier a zero signal is produced. When an inhomogeneity (depicted by the ellipse in Figure 4) is located within the bedding zone, the difference of the signals from both sides is amplified increasing the overall dynamic range for the detection of inhomogeneities.

During the measurement the antenna unit is rotated about 360° with an angular resolution of less than one degree. For suppression of surface reflection and a better coupling of the sounding waves into the pipe material, the antennas are pressed onto the inner wall of the pipe at a constant distance of 5 mm while rotating. In between crawler steps, the arrays can be retracted to avoid mechanical blocking in the pipe.

2.1.2. Electronic Unit

The electronic unit consists of the main radar parts like shown in Figure 1 and covers some additional electronics matched to the crawler application. This includes an optimised power supply (also for the stepping motor), a tilt sensor to keep track of the whole system's rotation between crawler steps, and control circuits for the regulation of the stepping motor and antenna lifting motor. Due to material properties of the bedding zone the bandwidth is limited to roughly 4 GHz. An RF-frontend was developed to allow switching between the two measurement modes (bistatic and bistatic differential).

2.1.3. Drive Assembly

As drive assembly a pneumatically driven crawler is used. It operates within a range of 5-7 bars air pressure which is generated outside the pipe and fed via air cables. Forward movement is stepwise with a step width of 2.5 cm. The position of the whole assembly is monitored by a distance sensor through a wheel encoder.

2.1.4. A typical measurement cycle

At the beginning the crawler fixes the position of the whole system by pressing his feet against the inner wall of the pipe. Than the tilt sensor delivers the current starting angle of the measurement. Next, the antennas are pressed onto the inner wall of the pipe by the lifting motor. After that the stepping motor rotates antenna unit and electronic unit about 360°. During this time, the radar collects its data and sends it to a PC platform for saving and a first visualization of the results. Next, the antennas are pulled down

again and the cycle is completed. To scan a whole pipe or section of it, the crawler is used to proceed the whole system forward or backward between each measurement cycle.

2.2. The Salt-Mine System

The problem of disaggregation around salt mine tunnels has been a known issue for years now. Up to now, there has not been any high-resolution method to assess the state of the disaggregation zone in a detailed manner. It consists of very thin gaps or small distributed cracks inside the salt rock. The actual crack distribution and possible preferred alignments of thin gaps is rather unknown to date. UWB radar provides a means to have a look inside the surface-near areas. The basic M-sequence system described earlier already has an impressive operational bandwidth of 4GHz in the baseband which is suitable to penetrate pipe or building materials as well as salt rock, etc. However, in order to detect very small targets of sub-cm or even sub-mm size, the RF properties of the radar needed further enhancements.

Simplified scattering models of typical targets in the disaggregation zone clearly indicate better interaction of very high frequencies with small distortions [1],[5]. Furthermore it has been shown, that frequencies up to 20GHz and even beyond travel through salt rock with acceptable attenuation.

Shifting the operational band of the M-sequence radar towards higher frequencies is a natural choice here, but it is not enough. Just as in the case of the tube crawler, the strongest signal components in the A-scans would be antenna coupling and the surface reflection. A differential operation mode like in the pipe inspection case is not feasible in salt mines. Thus, in order to separate weak reflections right behind the salt rock surface from its response, a high range resolution – and consequently a high measurement bandwidth – is a must.

Due to the very small size of disaggregation defects, their response to radar waves is overall very weak even if the surface reflection can be sufficiently well suppressed. It is therefore important to provide a large spurious-free dynamic range (SFDR) in order to avoid masking target responses by signal components coming from system imperfections. For example, calculations on a simple scattering model for a 1mm thin air gap in salt rock indicates that the backscattering of the target is more than 40dB below that of the surface reflection. In order to achieve high SFRD combined with a large bandwidth, proper calibration becomes mandatory. We adopted well-known calibration techniques from the area of vector network analysers for our salt mine system.

Since the spatial alignment of targets is rather unknown, polarisation of the sounding waves is also an issue. It is desirable to have polarimetric information for horizontal-, vertical-, and cross-polarisation alike. In summary of all mentioned requirements, the following modifications of the basic M-sequence concept have been implemented:

- Shifting & extending the operational bandwidth: the new system works from 1-13 GHz
- Increasing the equivalent sampling rate of the system from 9GHz to about 36GHz to be able to directly acquire the whole stimulus spectrum
- Using four receivers and directional couplers for parallel reflection (e.g. S11 and S22) and trans-mission measurements (e.g. S21 and S12)
- Attachment of an automated calibration frontend to remove system imperfections (increase SFDR)

Figure 5 below shows the resulting system diagram. The core RF-components from the basic system are shown in red. The system diagram resembles that of a common 2-port vector network analyser (VNA) with four internal receivers. In contrast to VNAs however, our UWB system works in the time domain stimulating and capturing all frequencies in the operational band at the same time.

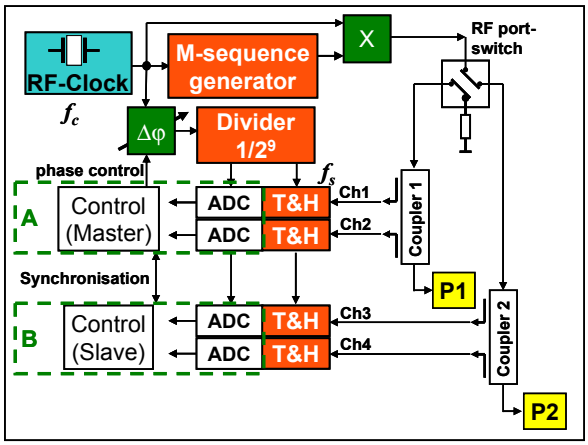

Figure 5: block diagram of new 12GHz bandwidth M-sequence UWB radar for salt mine inspection

The two measurement ports P1 and P2 are excited sequentially with the stimulus enabling the acquisition of all four S-parameters: S11 and S21 while P1 is active, S22 and S12 while port 2 is excited. The ports could be directly connected to the antennas. As mentioned before, we chose to include a frontend for automatic calibration as shown in Figure 6. The frontend holds a number of known calibration standards and connects the ports P1 and P2 to them as needed during calibration. During normal measurement operation, the horn antenna array is connected to P1 and P2. By acquiring all S-parameters, polarisation combinations HH and VV (both reflection measurements) as well as HV and VH (both transmission measurements) can be obtained.

The calibration procedures have been adopted from well-known VNA methods. There exist a vast number of possible solutions for full two-port calibration all with their specific advantages and

disadvantages. For the salt mine system, complicated calibration standards needing operator interaction were not feasible. The implemented frontend features simple coaxial standards, but still enables the use of different common algorithms: 12-term, 8-term, and even 16-term method can be used. For details on these methods (and others) the reader may consult [6].

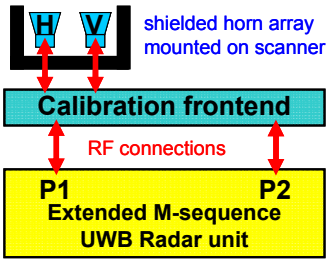

Figure 6: measurement ports and calibration frontend with horn antenna array

The application of such calibration methods require a high system stability and repeatability in order to make sense. These are inherent features of the M-sequence approach and have been kept also in the new system. In practical evaluations it turned out, that the 8-term method provided the best calibration results. For both reflection and transmission measurements, an SFDR in excess of 60dB has been reached after calibration [1]. Real-world measurements and results are shown in the next sections.

3. MEASUREMENT SCENARIOS

For proof of concept of the radar sensors, some practical measurement scenarios were tested. Example setups will be introduced here.

3.1. Sewer pipe test bed

In the case of pipe inspection, test beds with known distortions around concrete, stoneware and plastic (PVC-) pipes have been prepared and measured (see Figure 7 and Figure 8).

Figure 7: test bed with concrete, stoneware and plastic pipes before embedding them in sand.

Typical objects found in pipe beddings have been used as perturbations. Their arrangement can be taken from Figure 8 – copper cables (black lines), large stones (gray blocks), water (dark blue), air inclusions (light blue), wood (brown), and building rubble (dark brown) were placed on top and besides the pipes.

During the runtime of the project, six measurement campaigns were done in order to test and improve the prototype system step by step (including hardware, measurement software, and data processing algorithms).

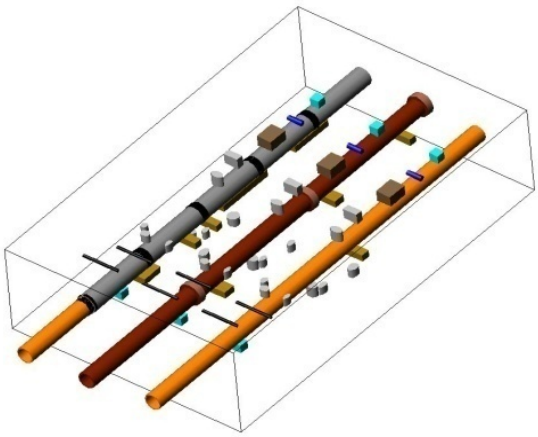

Figure 8: 3D drawing of the test bed with known perturbations.

3.2. Test measurements in salt mines

In the frame of the salt mine project, several measurements have been carried out throughout salt mines in Germany. In order to enable easy scanning and to be sure to have a pronounced disaggregation zone, old cylindrically shaped tunnels have been selected for investigation. First measurements were done to collect experience with the environment conditions in a mine as well as to find hints on what improvements the radar system would need. The final campaigns were carried out with a setup as shown in Figure 9 using the new 12GHz bandwidth radar with calibration frontend and a horn antenna array for polarimetric measurements. The antennas were scanned along the circumference of the tunnel surface to obtain a radargram of one slice. Then the trolley was moved along the tunnel axis a few cm and the next slice was acquired and so forth. It took about minute per radial scan and a tunnel section of 1m length has been scanned in 5cm steps. Since the radar setup scans contactless, its speed is far superior to other methods like ultra-sound, let alone classical gas-permeability measurements requiring bore holes. It should be noted though, that ultra sound measurements do have much better sensitivity to disaggregation compared to radar, since the wave propagation properties of salt and air are more different for sound waves than for radar waves.

Further measurements were conducted right after a new tunnel section was cut in the mine of Borth. The

setup was almost the same with the exception that scanning was done on a linear aperture along the tunnel ceiling. The goal of this measurement was to monitor the formation of the disaggregation zone of newly cut tunnels. The mine in Borth is about 900m below ground and known to show severe changes in the first few hours after cutting. The observation was conducted for a period of about 48 hours.

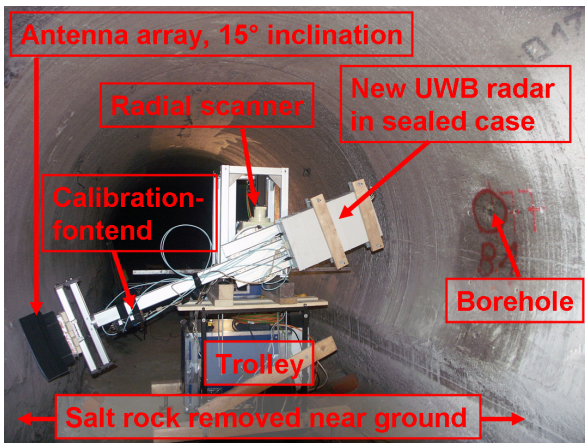

Figure 9: arrangement of new 12 GHz M-sequence radar system and scanner in the mine of Bernburg

4. MEASUREMENT RESULTS

Both applications not only require suitable radar systems, but also demand careful data processing to extract the wanted information. Since this paper emphasises the usefulness of M-sequence UWB radars in NDTCE, we only show examples of fully processed results.

4.1. Examples of tube crawler radar results

First the comparison of results from the two different measurement modes (bistatic mode and bistatic differential mode) of the tube crawler radar will be shown. Figure 10 depicts the radargram of one 360° slice of the plastic pipe in the standard bistatic measurement mode. In this case sample numbers are in range direction and stand for distance (the exact mapping depends on actual soil properties). Pixel colour corresponds to response amplitude. The strongest signal components appearing around sample 20 over the whole circle belong to the surface reflection and crosstalk of the antennas. Three inhomogeneities at angles of 90° and 270° can be identified as shown in Figure 10.

The bistatic differential mode results are depicted in Figure 11. It is obvious that the unwanted components around sample 20 are suppressed, but not 100% erased. The cancellation of antenna crosstalk and surface reflection is still imperfect due to asymmetries of the antennas and cable lengths, small fluctuations of the distance of the antenna pairs to the inner wall of the pipe, and inhomogeneous rotation during the measurement cycle. However, the strength of the three inhomogeneities' responses has been enhanced over the previous result. In the differential case, the signal from target one is amplified due to the fact that it is completely different from the antenna crosstalk, etc., which appears at a similar range (around sample 20).

Because of this modes' principle of taking the difference between two opposite antenna pairs, it cannot be said if a particular inhomogeneity is situated at the angle it appears or at the opposite side of the pipe. As can be seen from Figure 11, all the targets at 90° and 270° appear now at the same angle of 90°. Since target 1 and 3 have about the same distance to the pipe's wall, their responses melt into one bigger signal component. Thus, it is hard to distinguish targets from opposite sides of the pipe if they have the same distance. But it is still possible to draw conclusions about the homogeneity of the bedding zone – especially for very small distances from the pipe, which is the main purpose here.

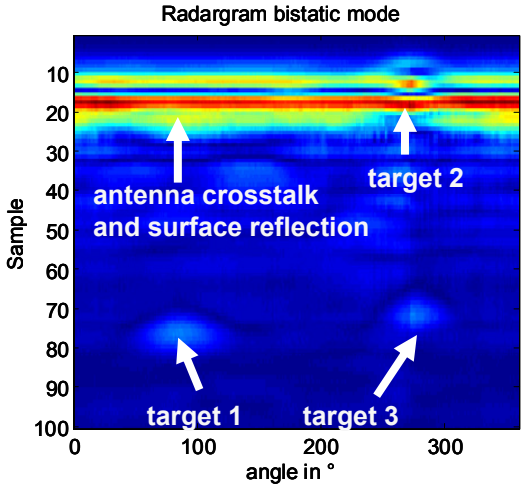

Figure 10: three inhomogeneities in the bedding zone detected with normal bistatic measurement mode

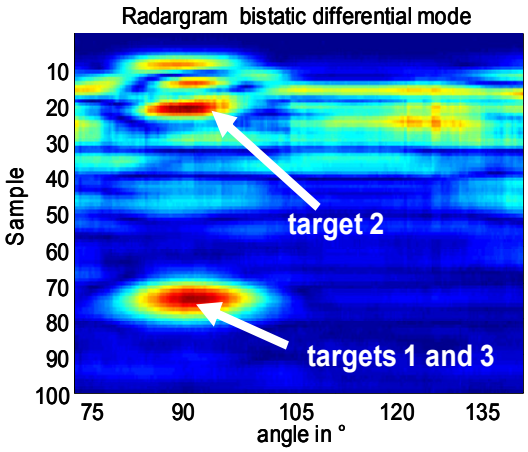

Figure 11: inhomogeneities in the bedding zone detected with differential bistatic mode

Figure 12 shows another result revealing four distortions near the top of a pipe. It shows a 3D-

volume view composed of many slices at a distance of 1.5 cm around a PVC-pipe. The anomalies seen are caused by a copper cable, building rubble, water inclusions, and an air gap. This kind of visualization is a large improvement to current pipe inspection systems because it allows a 3D view through the bedding zone around the pipe behind its wall.

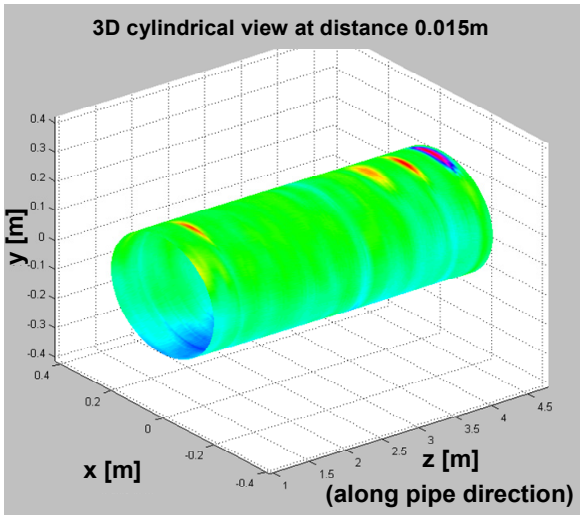

Figure 12: 3D view of distortions in a pipe's bedding: four anomalies 1.5 cm apart from a PVC-pipe.

4.2. Salt mine examples

As a first example, a radargram of one single scan performed in Bernburg is shown in Figure 13. The measurement setup and location is the one introduced in Figure 9. An angle of 0° corresponds to the antenna scanner arm being horizontal towards the borehole B1. The data shown was acquired through the vertically polarised horn antenna and represents a reflection measurement (i.e. S11). It has already been processed by several steps. At first, an 8-term calibration has been performed on the raw data to remove systematic imperfections of the radar and to flatten the system's frequency response. The next step involved removal of the antenna coupling as well as the surface reflection. Finally the data has been aligned to the salt rock surface, such that the Y-axis shows the distance inside the salt rock.

As can be seen in the highlighted area **A**, inhomogeneities appear almost throughout the whole scan but are especially strong near the ceiling. The removal of surface response was successful, but a few artefacts can still be identified.

The areas marked with **B** show distortions up to deeper depths inside the salt rock. As can be seen in Figure 9, the cylindrical shape of the tunnel has been broken by removing material in the ground regions. This leads to specially distributed forces inside the rock which seem to translate into stronger disaggregation.

Rather strong responses from inhomogeneities and probably even material layers could be observed especially in the ceiling region around 90°. The arrears **C** and **D** highlight such reflections. To get a better idea of the nature of these distortions, looking at a single scan might not be optimal.

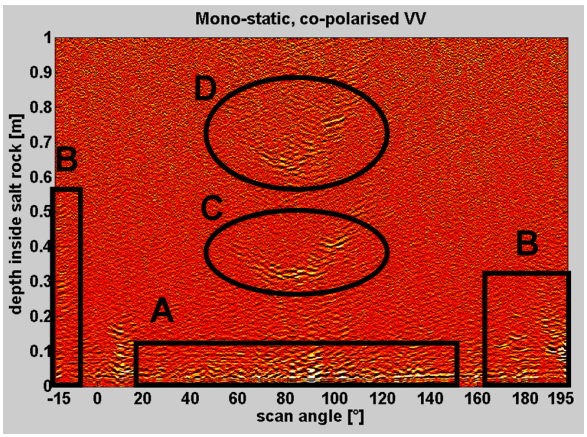

Figure 13: processed radargram of a single scan in the tunnel in Bernburg

Therefore, Figure 14 shows a 3D volume view of the disaggregation zone of the tunnel section around the scan presented before. This result has been composed from many slices taken along the tunnel axis, transforming the radargrams into the original cylindrical geometry, and enclosing volumes with significant reflectivity.

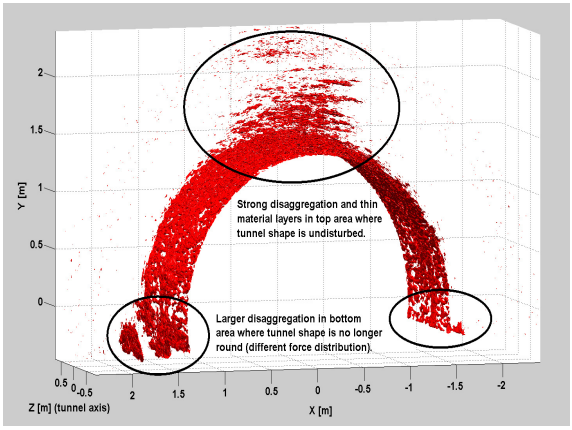

Figure 14: disaggregation around a 1m long salt rock tunnel section in Bernburg.

The results are in line with what was shown by the single scan before. Especially right behind the salt rock surface, distortions appear on the whole circumference. Please note that the surface reflection has been removed in the figure and all responses come from inside the salt rock. In the bottom region, strong disaggregation appears due to the distorted tunnel shape. Looking at the ceiling region from the sides reveals that the reflections there come from thin and flat material layers as well as from distributed inhomogeneities. It seems that the strongest signals of areas **C** & **D** in Figure 13 correspond to these layers.

As a last example a result from the measurement in Broth is presented in Figure 15. This time the antenna

array was moved along the ceiling of the tunnel with a linear scanner. Observation started only 6 hours after the new tunnel section in Borth was cut by the mining staff and was continued for about 48 hours. In order to see the development of the disaggregation zone in the fresh tunnel stub, the measurement results from an early scan at 6 hours after creation have been subtracted from a data taken at the end of observation time (54 hours after cutting the tunnel). The black line at the bottom of the picture indicates the original location of the salt rock surface. It's not visible since the plot shows the difference between two scans along identical locations. Right behind the surface, hints of built-up distortions can be seen, but especially in the area marked **A** (about 10-20 cm inside the salt rock), the structure has significantly changed within the two days.

Another interesting change can be identified in area **B** about 50 cm away from the ceiling. The X-axis of the plot points towards the entrance of the newly cut tunnel stub. The Entrance is at the position 3m. A stronger discrete crack started to form there, growing from the tunnel entrance towards the end of the stub. It should be noted, that the overall level of the responses collected in this measurement is much weaker than those from the old tunnel in Bernburg. That is why measurement noise and residual systematic errors, which could not be completely removed by calibration, are more prominent here.

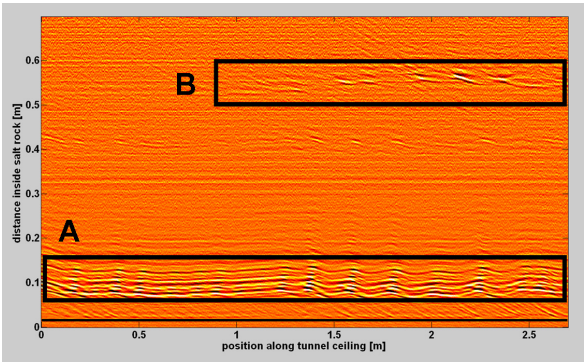

Figure 15: difference of processed radargrams along ceiling of a newly cut tunnel section after 6h and 48h.

5. SUMMARY

In this paper, we described two ultra wideband radar sensors based on a standard 4 GHz bandwidth M-sequence system. The introduced radars were matched to their specific applications with scanning antennas in a cylindrical measurement scenario. Both systems deal with high dynamic range problems to even detect smallest differences in the backscattered electro-magnetic waves. Besides other inspection methods, the sensors allow to look behind the surface and inside the materials in a contactless, non-destructive fashion resulting in a high measurement rate. Taking a full 360° scan in a sewer pipe will only take a few seconds; one scan in a salt mine tunnel was finished in a mere minute.

The proposed systems were evaluated and measurement results have been shown to accomplish the proof of concept. For ongoing research, the basic as well as new systems are subject to further developments in the NDTCE application sector.

6. ACKNOWLEDGEMENT

We would like to express our gratitude to all project partners involved in this work. Furthermore, the tube crawler project was supported by the German Federal Ministry of Economics and Technology (BMWi) under grant #16IN0338 and the salt mine project was funded by the German Federal Ministry of Education and Research (BMBF) under grant #2C1194.

7. REFERENCES

[1] R. Herrmann, J. Sachs, K. Schilling, F. Bonitz; "12-GHz Bandwidth M-Sequence Radar for Crack Detection and High Resolution Imaging"; GPR 2008: 12th International Conference on Ground Penetrating Radar; June 16-19, 2008; Birmingham, UK.

[2] F. Bonitz, M. Eidner, J. Sachs, R. Herrmann, H. Solas; "UWB-Radar-Sewer Tube Crawler"; GPR 2008: 12th International Conference on Ground Penetrating Radar; June 16-19, 2008; Birmingham, UK.

[3] F. Bonitz, J. Sachs, R. Herrmann, M. Eidner; "Radar Tube Crawler for Quality Assurance Measurements of Pipe Systems"; EURAD 2008: Proceedings of the 5th European Radar Conference; 27-31 October 2008; Amsterdam, The Netherlands.

[4] J. Sachs, P. Peyerl, S. Wöckel, M. Kmec, R. Herrmann, R. Zetik; "Liquid and moisture sensing by ultra-wideband pseudo-noise sequence signals"; Measurement Sci. Technol.; Vol. 14, 4th edition; pp. 1074-1087; 2007

[5] R. Herrmann, J. Sachs, P. Peyerl; "System evaluation of an M-sequence ultra wideband radar for crack detection in salt rock"; GPR2006: 11th International Conference on Ground Penetrating Radar; 2006; Columbus Ohio, USA

[6] D.K. Rytting; "Network analyzer error models and calibration methods"; RF & Microwave Measurements for Wireless Applications (ARFTG/ NIST); 1996